DATA ANALYSIS ON RESIDUAL STRESSES MEASURED IN CONCRETE BEAMS

Edward. H. Guo[1], Frank. Pecht[2], Lia. Ricalde[1], Donald. Barbagallo[2], Xinkai. Li[3]

Abstract
A core-ring strain gage (CRSG) test procedure has been devised for measuring the residual stress in a concrete pavement. Initially cantilevered concrete beams were selected for instrumentation to determine if beam stresses could be released and measured by drilling a core-ring. The known load induced stresses for a cantilever beam, before a core-ring is drilled, have a theoretical solution. At the same time, the known load induced stresses after a core-ring is drilled can be determined using numerical tools such as ABAQUS program. Other objectives of the beam tests were to determine an appropriate core-ring size, a range of core-ring depths, and the best spacing between the strain gage center and the core-ring edge to be used for future full scale tests. Most load induced strains were released after the core-ring depth reached 30 mm (1.2 inch). Although the comparison between calculated and tested results shows that a "blind-hole" model matches the test results well, the core-ring model still needs further study for more complicated cases. The results of the cantilever beam tests show a high potential for direct measurement of residual stress in concrete pavements for evaluation purposes.

Introduction

It is always important to recognize which stress causes a concrete slab to crack. In all existing airport pavement design procedures, a critical stress is first calculated under an assumed critical load using mechanistic models. The allowable load repetitions that lead to pavement failure can then be estimated using a "failure model" or a closed-form "transfer function." Therefore, it is important to find the most sensitive stress to pavement failure. Secondly, when an existing pavement needs to accommodate a heavy aircraft that was absent in the original design traffic mix, it is important to determine the magnitude of the critical stress induced by the aircraft.

The critical stresses in the above two examples are load-induced stresses which can be predicted using different models (Shoukry 2000). Load-induced stresses can also be well estimated from strains measurements by different types of strain gages (FAA NAPTF Web Site 2007, Guo et al. 2006(1)). Due to computational advances and assumption limitations, a good computer model will in many cases, but not always, predict stresses that closely match measured results (Guo 2006(2)). This correlation between calculated and measured stresses has been only verified for "load induced" stresses; i.e. those developed the first few seconds under a moving load. It has long been

[1] SRA International, 3120 Fire Road, Egg Harbor TWP, NJ 08234, USA. Tel 1-609-645-0900.
[2] Airport Technology Research and Development, Technical Center, FAA, Atlantic City, NJ 08405, USA. Tel. 1-609-485-8503.
[3] School of Transportation Science and Engineering, Harbin Institute of Technology, Harbin, 202 Haihe Road, Nangang District, Harbin 150090, P.R. China. Tel. 86-451-86282120.

recognized and verified by many recently published papers that concrete pavement cracking occurs not only due to traffic load. Some concrete pavements crack even before any traffic load is applied. During full scale testing in 2000 at the FAA's National Airport Pavement Test Facility (NAPTF) the test slabs cracked much earlier than predicted using existing pavement design model (Guo 2006(2)). Therefore, the "true" stress, which may be defined as "total" stress in the concrete pavement, must sometimes be significantly higher than the predicted or measured load induced critical stress. This is true because of "residual stress" which is defined as the existing stress in the concrete pavement before any load is applied (Guo 2005).

Several recently published papers provide with procedures to predict the "total stress" using 3-D or 2-D finite element (FE) models. These procedures consider residual stress due to temperature, moisture, creep and even build-in curling effects (Yu et al. 1998, Roa et al. 2005, Nam et al. 2007 and Rodden et al. 2007). Different assumptions based on laboratory test results studying the effects due to moisture and creep had been made. These procedures indicate progress of the research in this direction; however, the accuracy and precision of the procedures still need to be verified. As a first step, the residual stress in a concrete slab predicted by a model should be compared and evaluated against a directly measured value (if such a procedure is available).

A similar problem was encountered in structural engineering decades ago. Virtually all manufacturing and fabricating processes — casting, welding, machining, molding, heat treatment, etc. — introduced residual stresses into the manufactured object (Vishay Micro-Measurements Group 2007). The most widely technique used for measuring residual stress is the hole-drilling strain-gage (HDSG) method. The method consists in drilling a hole near a gage in the critical residual stress zone. The strain difference measured before and after the hole is drilled can be used to calculate the stress relaxation due to the hole; then the critical residual stress can be estimated in the structure before the hole was drilled. ASTM E837 provides detailed requirements for conducting the test and data analysis. Using this standard as the basis, a similar test procedure was developed to directly measure the residual stress in a concrete beam. The final objective is to develop a procedure for measuring residual stresses in concrete airport pavement slabs.

The study of the concrete beam residual stress, presented in this paper, was conducted in two stages. In stage one, the preliminary results from strain gage measurements made on loaded concrete beams before and after a core-ring is drilled in high stress zone are discussed (Pecht et al. 2008). Two conclusions have been reached: first, for a concrete mix with a maximum aggregate size no greater than 2.54 cm (1 inch), 30 mm (1.2 inch) or even 20 mm (0.8 inch) long strain gages are acceptable in acquiring accurate concrete strain data; second, the CRSG method provides significant strain changes nearby the ring. Major differences between the CRSG and HDSG procedures are discussed in Pecht et al. 2008.

The tests in stage two were conducted in November 2007 on two additional cantilevered beams. The cantilevered beams were loaded in bending to simulate the presence of residual surface stresses, and core-rings were then drilled to relieve the stresses. The cantilevered beam was selected for this study because the stress at any point can be easily calculated if the beam material is assumed uniform and linear elastic. However, it is difficult to approach the "uniformity" in a manually cast beam even if the

ASTM standard is strictly followed. Test data is presented in this paper to show how to minimize the effect of non-uniform elastic modules in residual stress measurement.

In the HDSG test procedure, the hole-size and hole-depth significantly influence strain changes. The strain change is also a function of spacing between the strain measurement point and the edge of the hole. The effects of the above three parameters are still significant in CRSG procedure. The first two effects are investigated in test stage two of the experiment and presented in this paper. Three core-ring diameters, (4.76, 7.62 10.16 mm, 2, 3 and 4 inch), and five core-ring depths (from 0 to 30 mm, 0 to 1.2 inch) were tested. The detailed effects of the third parameter will be studied in test stage three of the experiment and will be presented in a future paper.

Theoretical closed-form solutions are available for a "through hole" under uniform stress state in one direction (Kirsch 1989). Although the stress state is not completely the same to the test case, the equation is still helpful to understand the tendency of the parameter effects. Since no closed-form solution is available for a blind-hole, 3D FE analysis becomes a powerful tool to compare computational data with the obtained test data. Due to space limitation only one example is presented in this paper to qualitatively compare the results predicted by the 3D FE model and the beam test data.

The technique described in this paper has a high potential for practical use. The application of strain gages on a pavement surface is a convenient, fast and reliable procedure that has been successfully used at the FAA's NAPTF for several projects since 2002 (Guo et al. 2006(2)). After a gage is installed on a pavement surface, a core-ring can be drilled near by the gage. The measured strain change before and after the core-ring drilled, in conjunction with the 3D finite element analysis, can be used to determine the critical residual stress in the pavement. The entire testing procedure including gage installation, core-ring drilling and strain measurements can be completed within a few hours. The full scale test for measuring the residual stress at the FAA's NAPTF in a 4.6 m by 4.6 m (15 ft by 15 ft) curled slab, 30 cm (12 inches) thick has been completed in March 2008. The obtained results will be presented separately.

Beam Loading

The front and back views of the test setting are shown in Figure 1. During stage one of the testing it was found that "fixing" one end of the concrete beam was not easy. Therefore, in test stage two a new procedure was used to fix the beam end. The beam dimensions were 122 cm (4 feet) long and 15.2 cm (6 inches) in width and height. One end of the beam was fixed firmly under a very sturdy rail using a jack positioned under the beam end which provided a very strong support to the beam bottom. A uniformly distributed force was achieved placing a thin rubber sheet between the jack surface and the beam bottom, and between the rail bottom and the beam top. The back view of the test setting is shown in Figure 1(b).

A fork lift was used to hold a 1000 kg (2,200 lbs) steel plate above the steel bar. A second jack and a steel bar were positioned on the free end of the beam as presented in Figure 1(a). The second jack provided a load at the bottom of the steel plate while the reaction force being acted on the top of the free end of the beam. The reactive force was measured by a calibrated load cell. The maximum load used for testing never exceeded 185 kg (408 lbs). For applying the force exactly 7.62 cm (3 inch) from the free beam edge, the device shown in Figure 1(c) was positioned between the beam free end and the steel bar.

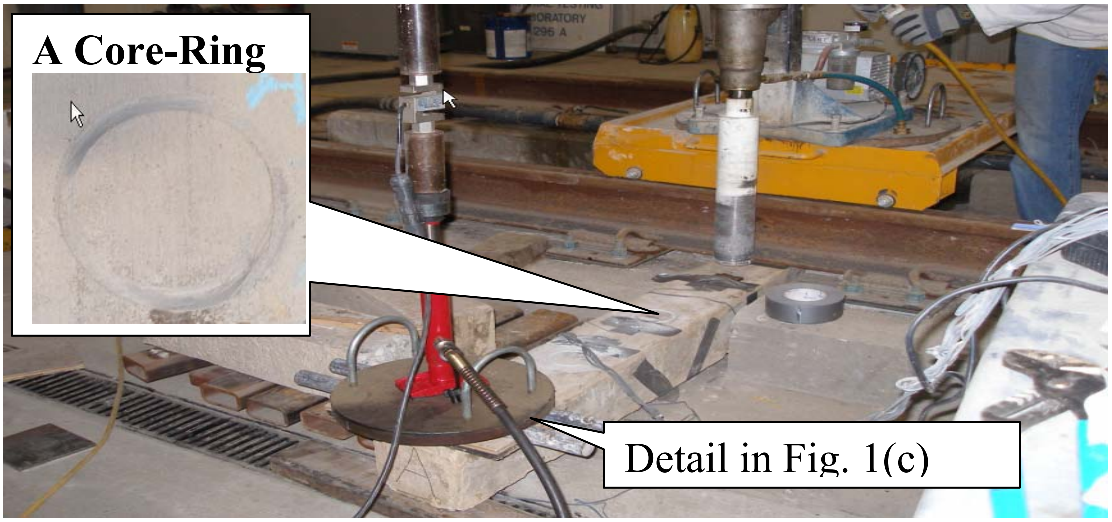

(a) A front view of the test – before the load is applied

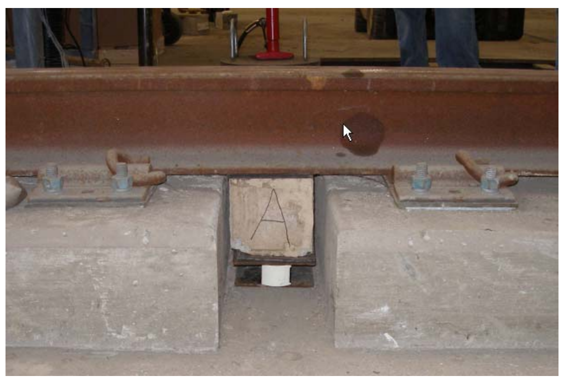

(b) A back view of the test

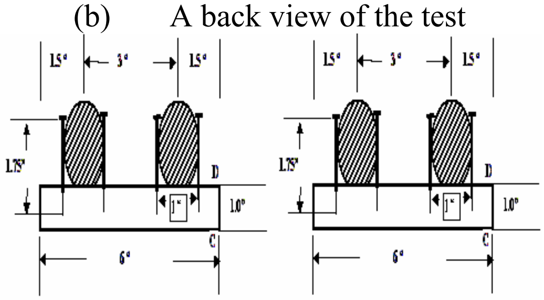

(c) Detail of Load Positioning Device

Figure 1 Testing Procedure

Uniformity of Elastic Moduli of the Concrete Beam

It is extremely difficult to manually cast a beam and reach uniform elastic moduli at the beam top and bottom; even when the specimens are cast following closely ASTM standards (Pecht et al. 2008). However, when using a simple equation to calculate the beam stresses at the top and bottom, the equation requires a uniform elastic moduli value.

Therefore, data for a beam before a core-ring was drilled was analyzed for selecting an appropriate beam position for testing.

Figure 2 presents the curves of strains vs. loads of beam B under two loading positions. Strain gages B2, B6, B7 and B8 were installed at all four sides along the longitudinal axis of the beam. In the first loading position, gage B2 was at the top and B6 at the bottom of the beam**,** the same as when it was cast and results are shown in Figure 2(a). For this loading case, gages B7 and B8 were at the two-side surfaces neutral axis of the beam. In the second loading position, the beam was rotated 90 degree around the beam's longitudinal axis, so gage B7 and B8 were at the beam top and bottom respectively while gages B2 and B6 were at the two sides of the beam. The results of the second loading position are presented in Figure 2(b). Each test was run twice to verify reliability and the elastic moduli was estimated using σ / ε, where ε is the measured load induced strain and σ can be calculated by following equation available in any text book of strength of materials:

$$\sigma = \frac{P \times L \times 6}{W \times H^2} \quad (1)$$

Where, P is the load, L is the spacing between centers of the load and the gage, W and H represent the width and height of the beam. Since all strain–load curves are approximately linear, the slopes in Figure 2 have been used to calculate the elastic moduli at the top, bottom and two side points of the beam. Results are presented in Table 1.

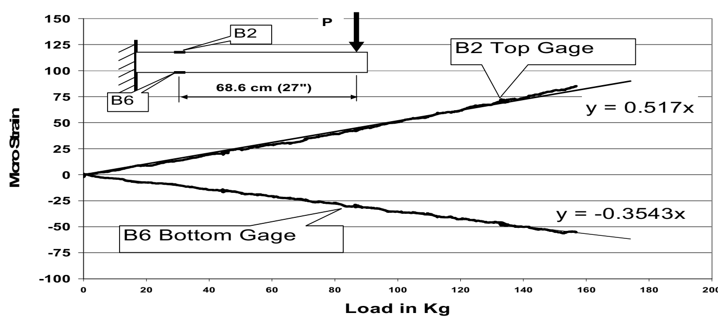

(a) Strain vs. load, gage B2 (Top) and B6 (Bottom)

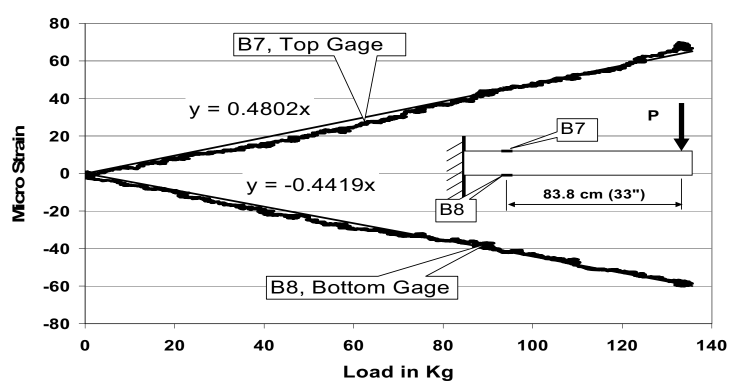

(b) Strain vs. load, Gage B7 (Top) and B8 (Bottom)

Figure 2 Strains vs. Loads for Two Beam Positions

Table 1. Calculated Elastic Modules Using Data from Different Gages, MPa (10^6 psi)

Gage ID.	B2	B6	B7	B8
First Test	22000 (3.20)	32150 (4.66)	29000 (4.20)	31500 (4.57)
Repeated Test	21800 (3.17)	31000 (4.50)	30000 (4.35)	28350 (4.11)
Average	21900 (3.18)	31600 (4.58)	29500 (4.28)	29900 (4.34)
Difference of E	30 - 43 % (bottom and top)		0.4 – 1.5 % (Side to side)	

For easy estimation of the surface stress in a cantilever beam, the material properties have been assumed to be uniform and the stress calculated using equation (1). However, the calculated moduli *E,* using data from gage B2 (top) and B6 (bottom), show a significant difference which conflicts with the assumption used for calculating the *E* values.

In the second loading position, gages 7 and 8 were on the top and bottom respectively. The calculated elastic moduli at the two side-points were very close. The results indicate that the manual casting the beam did not make the concrete elastic moduli uniform in the upper and lower portion but relatively uniform at the beam's neutral plane. For minimizing the error in analyzing the data, the appropriate beam position for testing should be with strain gages B7 and B8 on the top and bottom surfaces. Most of the data presented in this paper were collected from the tests with the beam in this position.

In 2004 at the FAA's NAPTF several dozens of beams, 50.8 cm (20 inches) long and 15.24 cm (6 inches) wide and high saw-cut from 30.5cm (12 inches) thick concrete slabs, were tested in the laboratory for measuring flexural strength. The tests followed strictly ASTM C78. Different beam positions were tested: the beam top and bottom were selected randomly using the slab top, middle and bottom. The flexural strengths of all groups were statistically similar. In 2006, several beams of similar size as described above were cast using the same concrete mix used for casting the 122 cm (4 feet) beam for this residual stress study. It was also found that the elastic moduli at the beam top and bottom were significantly different; however, their flexural strengths were still similar at about 4.15 MPa (600 psi) for all the specimens. In all concrete pavements design procedures, pavement life is more sensitive to concrete flexural strength than concrete elastic moduli. However, the critical stress in a full scale testing pavement is proportional to the elastic moduli (assumed or measured) since the stress must be calculated using the measured strain. Therefore, it is more important selecting appropriate concrete elastic moduli for full scale test data analysis than for pavement design.

Test Procedure and Typical Results

Two 122 cm (4 feet) long beams were tested. Fourteen sensors were installed at the beam top and bottom and one sensor was at the surface of the beam sides. The beam was fixed at one end as described previously, the loading device including a plate and steel bar were positioned appropriately to make the loading center 7.64 cm (3 inch) from the beam end edge (Figure 1(c)). At that moment, stresses were developed due to the weight of the loading device and the beam self-weight. The data collection system was set at zero before additional load was applied. The measured strain after the load was applied corresponded to the load induced strain. Before a core-ring was drilled, the beam was loaded up to about 181.6 kg (400 lbs) with target load increments of 45.4 kg (100 lbs). Since the load was applied by a manually operated jack, the loading process was very slow. When the load reading reached the target value, in the computer monitoring screen, the load was held for about 5 seconds, and then increased to the next step. After the load reached its maximum, the jack was released so the load quickly dropped to zero. Data system recorded the strains and loads for the entire loading and unloading period.

Tests were planned for studying the effects of five core-ring depths, including the first one before a core-ring was drilled. Two types of tests were conducted. The first was a continuous process for all core-ring depths saving the record of the entire test process into a single file. As mentioned previously, the data system was turned on and incremental loads were applied until it reached the maximum target value of 136.2 kg, (300 lbs). Then a shallow core-ring was drilled and the depth was measured and recorded while the load was held. The ring was continuously drilled to reach the next depth and measured, until all planned depths were completed. Then the load was removed and the data collection system was turned off.

The advantage of this test procedure was to use a unique reference for all core-ring depths. Analysis of the results would be more accurate and easier to compare. The strain records of gage A9 and the loads vs. time curves in beam "A" test are presented in Figure 3. The load reached the target value of 136.2 kg (300 lbs) in two load increments due to manually controlled jack malfunction. The load reached the target two load increments in only one step. After a core-ring was drilled to 1.27mm (50 mils), the strain of A9 dropped down from 70 to 60 micro strains. After the next drilling the core-ring depth reached 3.81 mm (150 mils), and the strain dropped down to about 45 micro strains. The records for the next two drillings were not stable so they are not presented in Figure 4.

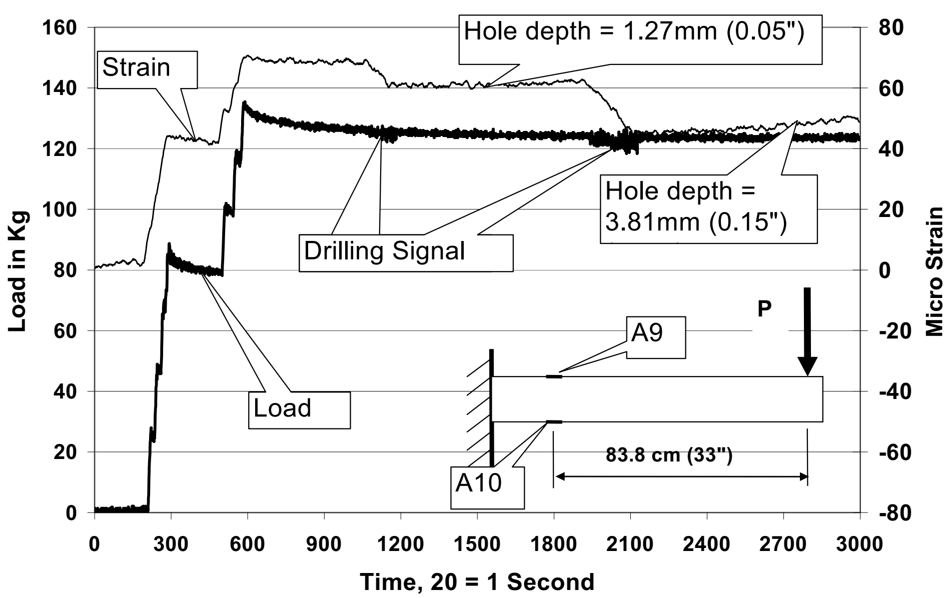

Figure 3 Core-ring Depth Effects in Continued Drilling Process

The second type of test procedure divided the study of core-ring depths into five tests and the data was recorded into five separate files. The first step was the same as the procedure stated in the first paragraph of this section. The second step started by drilling a shallow core-ring while the data collection system was off.

Then the data collection system was turned on and followed the same procedure in the first step. The drilling continued until it reached the second target depth, then the data system was turned on. The same loading procedure was followed and the data recorded.

The advantage of this procedure is easy to control the test stability and quality. The disadvantage is that each test has its own initial reference point and the data of five tests has to be evaluated based on five different references so unexpected errors may be introduced in the analysis by the loading device re-setting for each test.

The beam top and bottom strains and the loads collected by gages B7 and B8 in test steps 1, 3 and 5 are presented in Figure 4. The gage length of B7 was 20 mm (0.8 inch). A 10.2 mm (0.4 inch) core-ring was drilled near gage B7 with spacing 15 mm (0.6 inch, gage center to the ring edge). The maximum strains of gage B8 saw no significant change in the three tests but the maximum top strains of gage B7, 15 mm (0.6 inch) from the core-ring edge dropped from about 70 micro strain down to 35 and then down to 15 micro strain. It was therefore verified that the strain measured nearby a drilled core-ring is sensitive to the drilled depth of the ring. Therefore, this testing procedure could also have a high potential to release the residual stress in a concrete pavement.

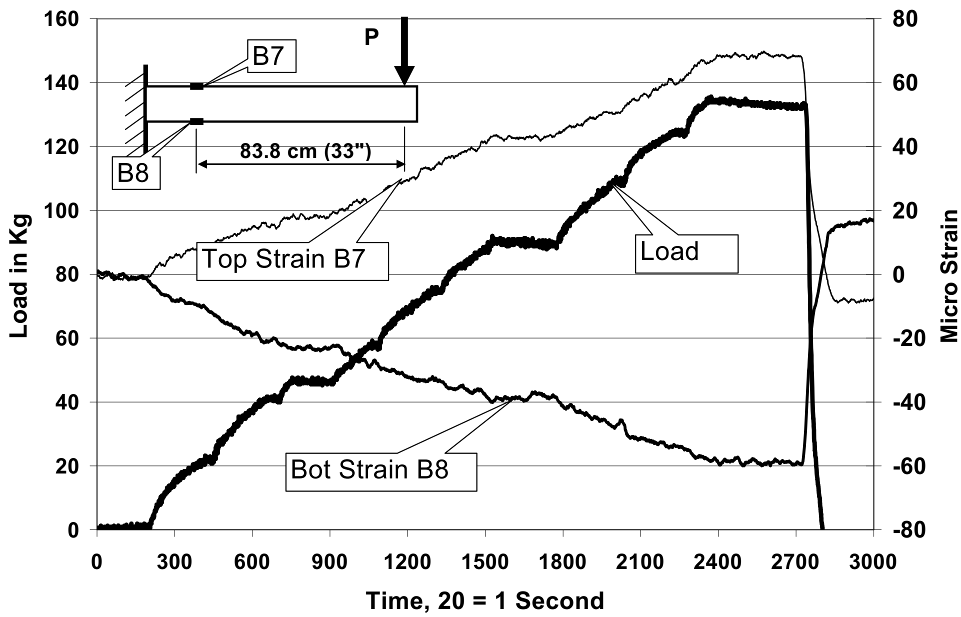

(a) **Before a core-ring was drilled**

Figure 4 Top and Bottom Strains and Loads

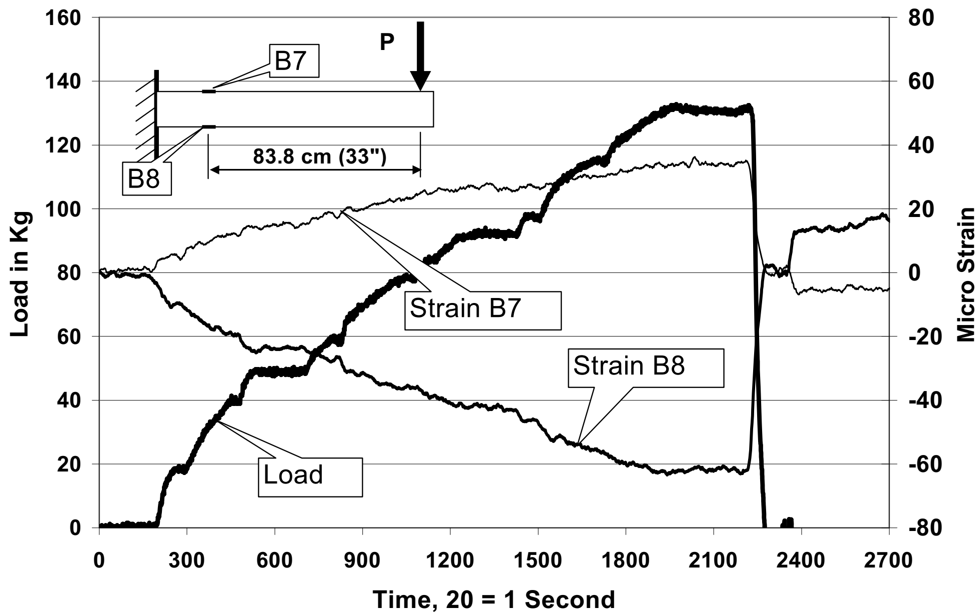

(b) After a 16 mm depth core-ring was drilled

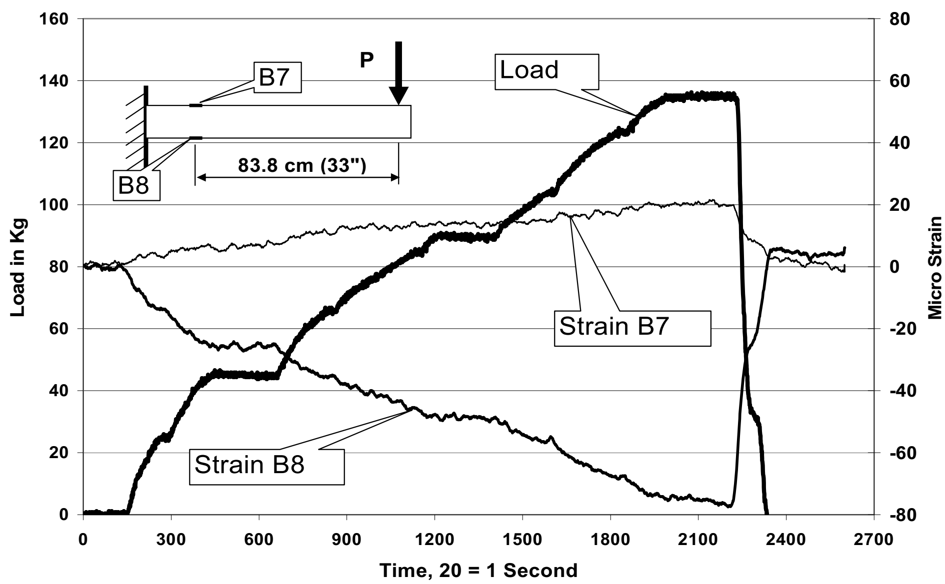

(c) After a 30 mm (1.18 inches) depth core-ring was drilled
Figure 4 Top and Bottom Strains and Loads (continued)

Analysis of the Results

Theoretical Solution

The stress distribution around a circular hole in a plate subjected to uniform tension in one direction was analyzed by G. Firsch in 1898 and the closed-form solution can be found in Vishay Micro-Measurements Group, 2007. Figure 5 presents the effect of hole-size on the convergence rate of radial stresses. The drilled hole is in full depth rather than a blind one, and uniform stress state is also different from the state in the tested beam.

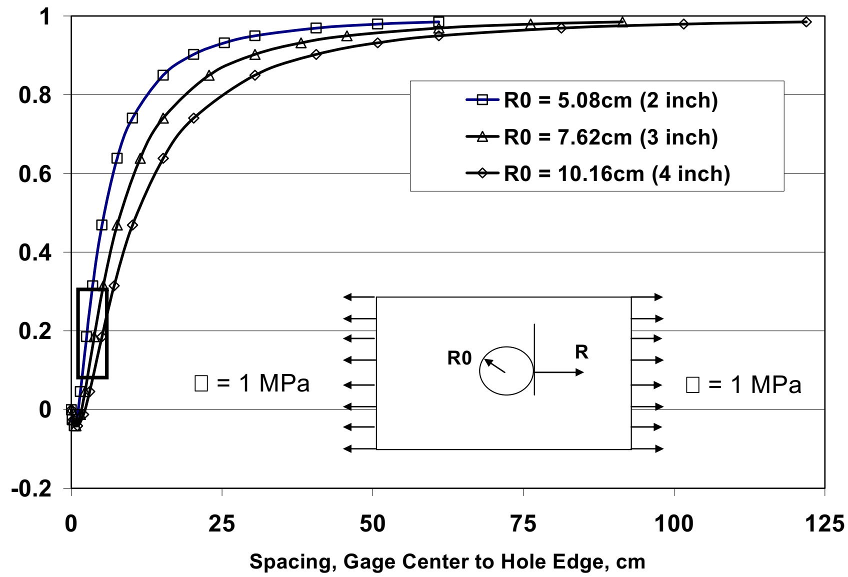

Figure 5 Radial Stress vs. Gage Spacing to the Hole Edge – Effects of Hole Size

However, the validity of equation (1) is based on several assumptions (Timoshenko 1953). If the same assumptions are accepted, a thin, unit thick layer at the top of the cantilever beam can be cut and defined as a free body. The two stress-states, theoretical and tested, are relatively similar since the shear stress acting on the free body and the normal stress difference through the thickness are small. Therefore, Firsch's results are used in this paper to discuss the concepts. For straight forward comparison, the uniform stress is assumed 1 MPa (145 psi), and hole sizes are 4.76, 7.62 and 10.16 cm (2, 3 and 4 inches). The radial stress distributions are presented in Figure 5 after a full depth hole is drilled.

First, the smaller the hole the quicker the strains converge to the stress without hole. Second, the objective of the study is taking advantage of the stress relaxation correlated to the decrease of measured strain which allows the estimation of the residual stress before a hole is drilled. Therefore, the gage should not be placed too far from the hole. Also, the gage should not be placed too close to the edge of the hole, because within a very small area the stresses are negative. This could lead to confusion during data analysis. If the target stress-drop is 70 to 90 % of the non-hole stress, the gage position for measuring the strain variation should be within the distance indicated by the rectangular zone in Figure 6. Third, the results of a 5.08 cm (2 inches) diameter hole vary the quickest among the three diameters and could introduce maximum error in measurement. Therefore 2.5 to 5 cm (1 to 2 inch) and 3.5 to 7 cm (1.35 to 2.75 inch) gage spacing should be used for holes with diameter 7.6 or 10.2 cm (3 or 4 inch) for next step tests.

The Effects of the Core-ring Size and Depth
For investigating the effects of core-ring size and depth, results of thirty tests (fifteen tests plus fifteen tests repeated) are organized and presented in Figures 6 to 8. The continuous test procedure (type one) did not provide results covering all planned core-ring depths (only the first two in Figure 3). Therefore, the results received from the second type of tests are used in the analysis. Although the maximum load for each test was controlled as close to the target of 136.2 kg (300 lbs) as possible, there were still slight differences in the applied loads. Therefore, all strain results have been normalized for comparison (multiply by target load and divided by recorded load). Since all tests were repeated, results for both are presented to verify test reliability.

The strains vs. five core-ring depths for a 4.76 cm, 7.62 cm and 10.2 cm (1.875, 3 and 4 inch) diameter core-ring are presented in Figures 6, 7 and 8 respectively. Findings are summarized below:

(1) All strains near a core-ring varied through depth at top of the beam but the bottom strains remained almost constant;

(2) The strains nearby the smallest core-ring 4.76 cm (1.875 inch) diameter converged faster than the other two. The findings are similar to those in Figure 5 obtained by theoretical analysis. For successfully measuring the residual stress in concrete pavement, it is desired to measure large stress relaxation with a relatively shallow core-ring. Therefore, the diameter size of 4.76 cm (1.875 inch) core-ring will not be recommended for future testing;

(3) The relative strain reductions ($\square_{min}$ / $\square_{max}$) in Figures 7 and 8 for a core-ring depth of 15 mm (0.6 inch) are similar (46% vs. 50%). When the depth was increased, both strains received higher reductions. The effects of spacing between the gage center and the core-ring edge will be investigated in detail during the next stage of testing.

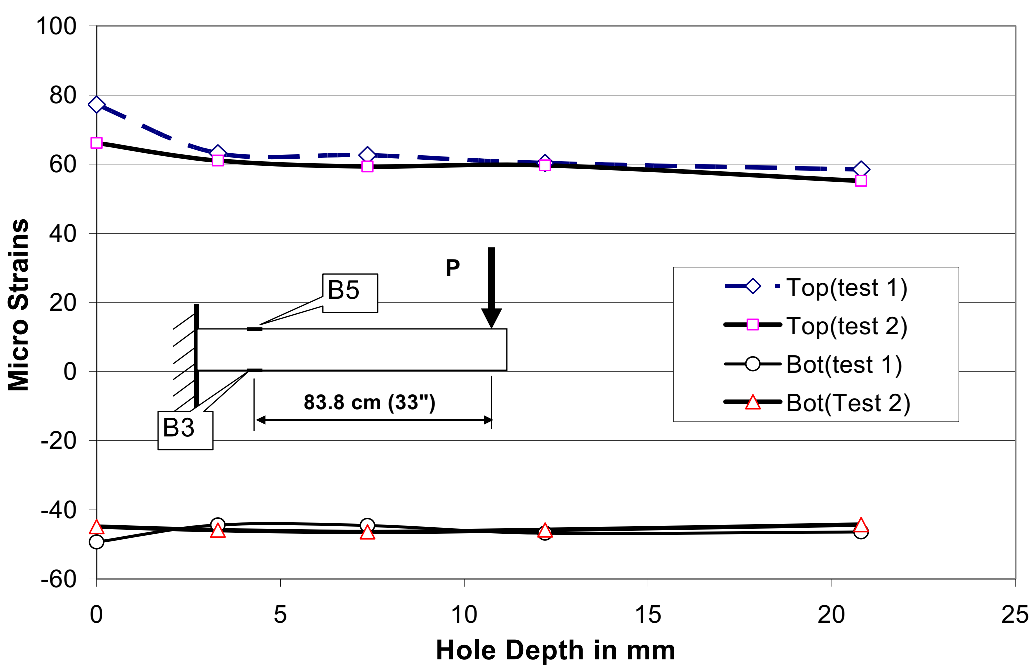

Figure 6 Strains vs. Core-Ring Depths, Diameter = 4.76 cm (1.875 inches), gage center to ring edge = 4.76cm (1.875 inches)

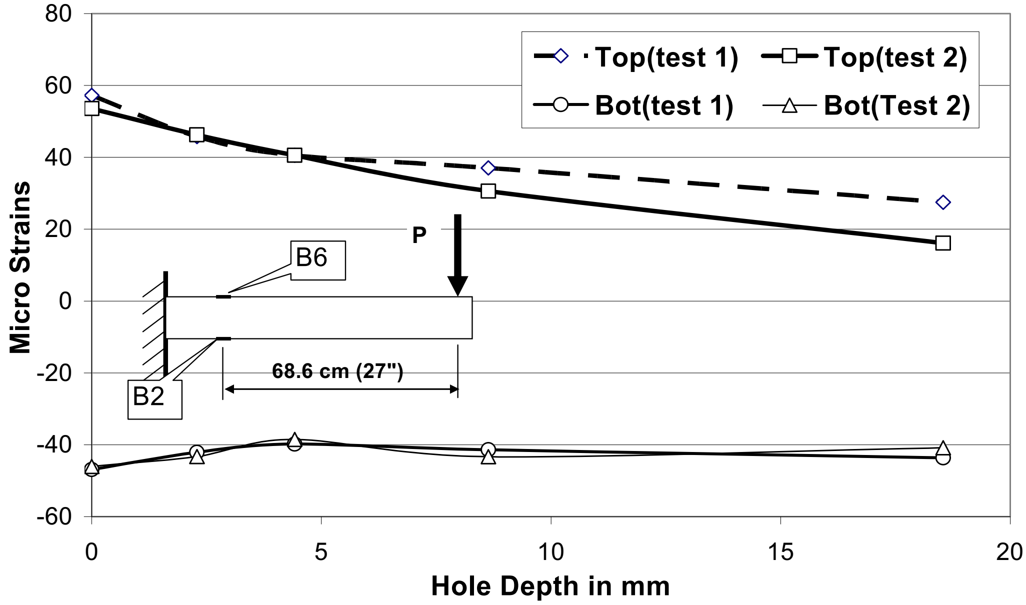

Figure 7 Strains vs. Core-ring Depths, Diameter = 7.62 cm (3 inches), Gage center to ring edge = 19 mm (0.75 inches)

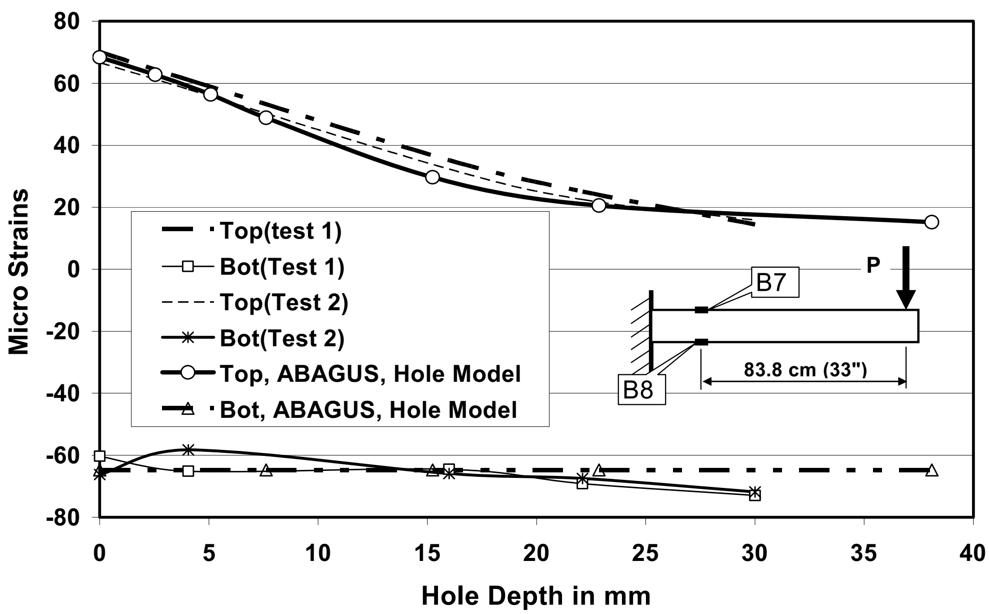

Figure 8 Strains vs. Core-Ring Depths, Diameter =10.2 cm (4 inches), Gage Center to Ring Edge = 22 mm (0.875 inches)

3D Finite Element Results

The beam test has been simulated using 3D finite element program ABAQUS. The element meshes, radial stresses before and after a 7.62cm (3 inch) core-ring was drilled are presented in Figure 9. The results of a fixed-end beam before a core-ring was drilled match well the results obtained using Equation (1). After a hole is drilled, the stresses within a small area near the core-ring edge and along the beam longitudinal axis decrease significantly. The strain drop was more significant between the core-ring and the load as shown in Figure 9(c). Therefore, the core-ring should be drilled at the other side of the gage rather than between the gage and the load.

The detailed calculated stress variation at the beam top and bottom after a 10.2 cm (4 inch) core-ring was drilled are presented in Figure 8 for comparison with the obtained test data. It can be seen that the ABAQUS calculated strains match the test data well. However, it is important to notice the differences between the “core-ring” in the test (Figure 1(a)) and the “hole” in the 3D FE program (Figure 9(a)) though both are blind and have the same depth. The core-ring model is still recommended for further study until the differences between the core-ring and blind-hole models are fully understood.

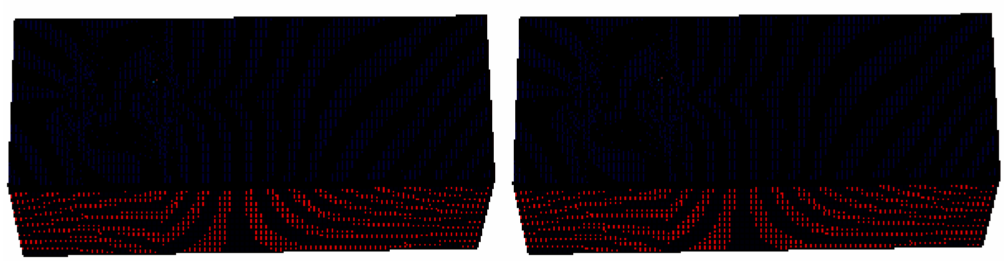

(a) Finite Elements after a Hole is Drilled

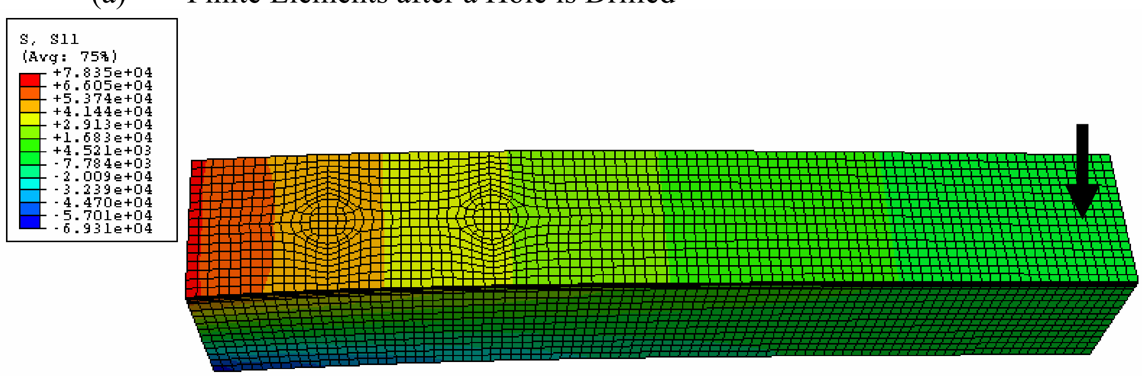

(b) Radial Stresses Before a Hole is Drilled

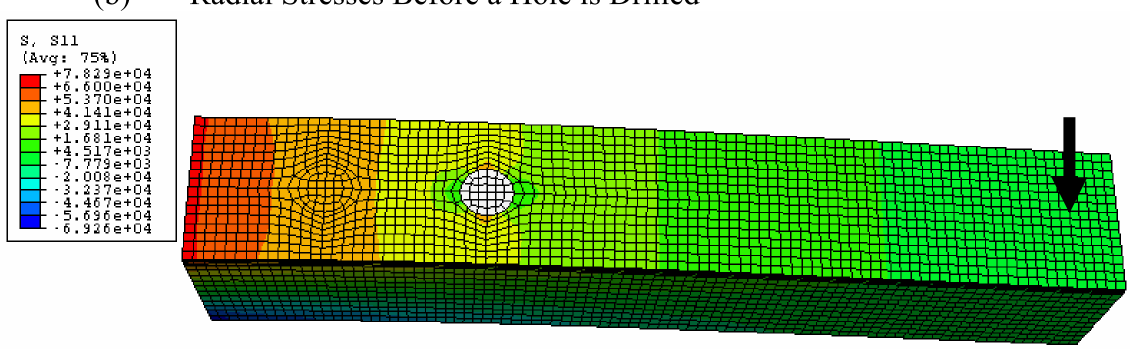

(c) Radial Stresses after a Hole is drilled

Figure 9 3D Radial Stress Results Calculated using ABAQUS

Conclusions

The core-ring strain gage test procedure, developed during testing of cantilevered concrete beams, shows a high potential to be used for direct measurement of the residual stress in concrete pavements for evaluation purposes. Core-ring diameters of 7.6 and 10.2 cm (3 and 4 inch) and 2.5 to 7 cm (1 to 2.75 inch) spacing between the gage center and the core-ring edge are recommended for use in future full scale pavement testing. The analysis using theoretical and 3D FE numerical models support the above findings. Specifications for using the CRSG method in engineering practice still have a long way to go; they should be developed using a 3D FE program, along with an appropriately selected model (the blind hole or core-ring), and in conjunction with full scale test data.

Acknowledgement

This work was supported by the FAA Airport Technology Research and Development Branch, Manager, Dr. Satish K. Agrawal. Special thanks are given to Dr. Gordon F. Hayhoe for his technical leadership in test planning and organization and to Mr. Chuck Teubert for his test management. The first author would also like to express his appreciation to Professor Xinshen Lu, Jiaotong University, China, for discussing the potential of stress release procedure in ship manufacturing which he has been familiar with for decades. The contents of the paper reflect the views of the authors, who are responsible for the facts and accuracy of the data presented within. The contents do not necessarily reflect the official views and policies of the FAA. The paper does not constitute a standard, specification, or regulation.

References

ASTM C 78-94 (1994). "*Standard Test Method for Flexural Strength of Concrete"* (Using Simple Beam with Third-Point Loading)

ASTM E837-01 (2001). "*Standard Test Method for Determining Residual Stresses by the Hole-Drilling Strain-Gage Method.*"

FAA NAPTF Web Site (2007). http://www.airporttech.tc.faa.gov/naptf/

Guo, E. H, Dong, M. M. and Daiutolo, H. (2005). "*Curling under Different Environmental Variations as Monitored in a Single Concrete Slab*," Proceeding of the 7th International Conference on Concrete Pavements, page 1189 – 1203, Colorado Spring, Colorado.

Guo, E. and Pecht, F. (2006(1)) *"Critical Gear Configuration and Positions for Rigid Airport Pavements – Observation and Analysis,"* Geotechnical Special Publication No. 154, Pavement Mechanics and Performance, page 4-14, ASCE, June 2006.

Guo, E. (2006(2)). "*Fundamental Modeling of Curling Responses in Concrete Pavement*" 6th International DUT-Workshop on Fundamental Modeling of Design and Performance of Concrete Pavements, Belgium, September, 2006

Kirsch (1989). VDI, Volume 42. See Reference by Timoshenko 1953, page 407.

Nam, J. H., Kim, D. H., Choi, S., Won, M. C. (2007). "*Variation of Crack Width over Time in Continuously Reinforced Concrete Pavement,"* TRB 2007 Annual Meeting CD-ROM.

Pecht, F. and Guo, E. (2008). "*Core-Ring Strain Gage Procedure for Measuring Residual Stress in A Concrete Beam,"* to be presented in 6th International Conference on Road and Airfield Pavement Technology, July 20-23, 2008.

Rao, S., Roesler, J.R. (2005). *"Characterizing Effective Built-In Curling from Concrete Pavement Field Measurements,"* Journal of Transportation Engineering, Volume 131, Issue 4, page 320-327, April 2005

Rodden, R., Roesler, J.R. and Lange, D.A. (2007). "*A Micromechanical Approach to Computing Linear and Nonlinear Moisture and Temperature Stresses in Concrete Pavements,*" International Conference: Advanced Characterization of Pavement and Soil Engineering Materials, 20-22 June 2007, Athens, Greece,

Shoukry, S.N. (2000). (Edited) "*Finite Element Modeling of Pavement Structures*", Proceddings of the Second International Symposium on 3D Finite Element for Pavement Anlaysis, Design and Research"

Timoshenko, S.P. (1953). *"History of Strength of Materials,"* McGraw-Hill Book Company, New York, 1953.

Vishay Micro-Measurements Group (2007). "*Measurement of Residual Stresses by the Hole-Drilling Strain gage Method,*" Website: http://www.intertechnology.com/Vishay /pdfs/TechNotes_TechTips/TN-503.pdf

Yu, H. T., Khazanovich, L., Darter, M. and Ardani, A. (1998). "*Analysis of Concrete Pavement Responses to Temperature and Wheel Loads Measured from Instrumented Slabs,*" TRB Journal Volume 1639, page 94-101, 1998.